Journal of Thermal Analysis and Calorimetry, Vol. 57 (1999) 717-736

GLASSFORMER FRAGILITIES AND LANDSCAPE EXCITATION PROFILES BY SIMPLE CALORIMETRIC AND THEORETICAL METHODS

C. A. Angell, J. L. Green, K. Ito, P. Lucas and B. E. Richards

Department of Chemistry, Arizona State University, Tempe, AZ 85287, USA

Abstract

In this paper we introduce two key notions related to understanding the 'glassy state' problem. One is the notion of the 'excitation profile' for an amorphous system, and the other is the notion of the 'simple glassformer'. The attributes of the latter may be used, in quite different ways, to calculate and characterize the former. The excitation profile itself directly reflects the combined phonon/configuron density of states, which in turn determines the liquid fragility. In effect, we are examining the equivalent, for liquids, of the low temperature Einstein-Debye regime for solids though, in the liquid heat capacity case, there is no equivalent of the Dulong/Pettit classical limit for solids.

To quantify these notions we apply simple calorimetric methods in a novel manner. First we use DTA techniques to define some glass-forming systems that are molecularly simpler than any described before, including cases which are 80 mol% CS_2, or 100% S_2Cl_2. We then use the same data to obtain the fragility of these simple systems by a new approach, the 'reduced glass transition width' method. This method will be justified using data on a wider variety of well characterized glassformers, for which the unambiguous $F_{1/2}$ fragility measures are available. We also describe a new DTA method for obtaining $F_{1/2}$ fragilities in a single scan. We draw surprising conclusions about the fragility of the simplest molecular glassformers, the mixed LJ glasses, which have been much studied by molecular dynamics computer simulation.

These ideas are then applied to a different kind of simple glass – one whose thermodynamics is dominated by breaking and making of covalent bonds – for which case the excitation profile can be straight-forwardly modeled. Comparisons with the profile obtained from computer studies of the molecularly simple glasses are made, and the differences in profiles implied for strong *vs*. fragile systems are discussed. The origin of fragility in the relation between the vibrational and configurational densities of states is discussed, and the conditions under which high fragility can convert to a first order liquid-liquid transition, is outlined.

Keywords: chalcogenides, dielectric relaxation, excitations, fragility, glassformer

1. Introduction

Liquids exhibit a wide variety of responses to changes in temperature and pressure, ranging from very rapid to very slow. This is particularly brought out when data are examined for corresponding states based on some appropriate scaling of temperature to account for the different particle interactions [1]. These changes can be

1418–2874/99/ $ 5.00

Akadémiai Kiadó, Budapest
Kluwer Academic Publishers, Dordrecht

associated with differences in the fundamental nature of configurational excitations which the liquid can sustain. To understand better the behavior of viscous liquids we have recently characterized liquids in terms of their 'excitation profiles' which reflect the density of configurational states characteristic of the liquid. The excitation of these states, with concomitant buildup of heat capacity, in the low temperature regime of liquids provides a parallel with the excitation of phonons and heat capacity in the low temperature (Einstein-Debye) regime of solids.

The upper portion of what we are calling the excitation profile was presented recently [2] for a mixed LJ system as the energy of the 'inherent structures' *vs*. the temperature at which the system had been equilibrated (prior to the quench procedure which identifies the potential energy of the inherent structure [3]). The inherent structure energy is the potential energy of the structure to which the system has been driven by the *TS* term in the Helmholz free energy $A=E-TS$ which the system must minimize in order to be in thermal equilibrium at the temperature *T*. The lower portion of the profile cannot be 'seen' by simulations because of the intervention of the glass transition for the simulated system. This occurs when the structural relaxation time for the temperature in question exceeds the computer time available for the study [4] (currently about 10 ns). A smaller portion of this same profile was presented for the case of a one component LJ system more than a decade ago [5], when the available time was only about 10 ps. We can complete the excitation profile presented by Sastry *et al*. using the value of T_c of the Mode Coupling theory obtained by Kob and Andersen [6] for the mixed LJ system, and the observation that T_c/T_K (T_K the ground state temperature) for systems of comparable character is ~1.6 (see below). This excitation profile is shown in Fig. l.

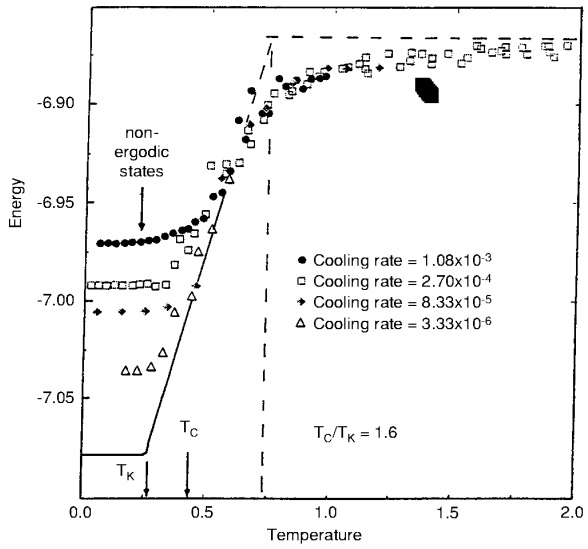

Fig. 1 The configuron 'excitation profile' for a system of mixed LJ particles, based on the inherent structure *vs*. energy determinations for this system obtained from assessments using different cooling rates (see legend) and extrapolating to infinitely small cooling rates using the observation based on data for moderately fragile liquids that T_c/T_K ~1.6 [8]

The profile of Fig. 1 shows a singularity on arrival at the ground state, as is usually envisaged in discussion of the Kauzmann temperature [7]. However there is no need for this, as will be emphasized later. The temperature T_c occurs less than halfway to the 'top of the landscape', in contrast to the expectation expressed by one of us for fragile liquids [8]. Since it has always seemed natural to expect the simple mixed atom liquids to be very fragile this is a matter for concern. We will therefore first address the question of simple molecular glassformer behavior to see whether the expectations of fragile behavior for LJ and mixed LJ is a valid one.

2. Simple glassformers

In this paper we give attention to two types of simple glassformers – those that are simple by virtue of their molecular simplicity, and those that are simple by virtue of the dominance of a single type of interaction, particularly a covalent bond.

2.1. Molecularly simple glassformers

Simply constituted glassformers are uncommon because most simple molecules have little difficulty in finding an efficient packing which guarantees that melting at T_m will only occur when the product $T\Delta S$ needed to overcome the energetic advantage of the crystal over amorphous packing ΔH, occurs when T is not far from the boiling point, T_b. The hot liquid is highly fluid, and crystallization on cooling below T_m occurs very readily. However, there are a few molecules which happen to have shapes and/or atomic size relations for which no very efficient packing exists, and then the melting condition is met when $T<<T_B$. The melt is then viscous at T_m, crystal nucleation is slow and crystal growth is inhibited i.e. glasses form [9]. Empirically it is found that this is common if the system meets the condition $T_b/T_m \geq 2.0$. The 3-atom molecule CS_2 is on the borderline by this criterion, T_b/T_m,=1.97, while the four-atom molecule S_2Cl_2 (T_b/T_m=2.09) is a 'good' glassformer. 15% of S_2Cl_2 in a CS_2+S_2Cl_2 mixture proves sufficient to permit vitrification of small samples [10].

The glass transition temperatures for solutions in this system are shown in Fig. 2 which contains also the approximate phase diagram. The variation in T_g is linear, suggesting ideal solution behavior. This contrasts with the behavior in the system CS_2+toluene [11] which shows strongly curvilinear behavior over the same glassforming solution range but still yields the same extrapolated T_g for pure CS_2, namely, 92 K.

The fragilities of the pure components CS_2 and S_2Cl_2 may now be estimated in either of two ways. Firstly the limited viscosity data available [12] may be compared with those of other liquids on a T_g-scaled basis [13, 14] – which gives only qualitative information but shows that both liquids are less fragile than, for instance, the well-studied case of orthoterphenyl [13]. Secondly, the fragility can be obtained semi-quantitatively from the reduced width of the glass transition as demonstrated recently for molecular liquids [15], and as can be demonstrated for inorganic network liquids from the T_g width *vs.* viscosity activation energy correlation of Moynihan [16].

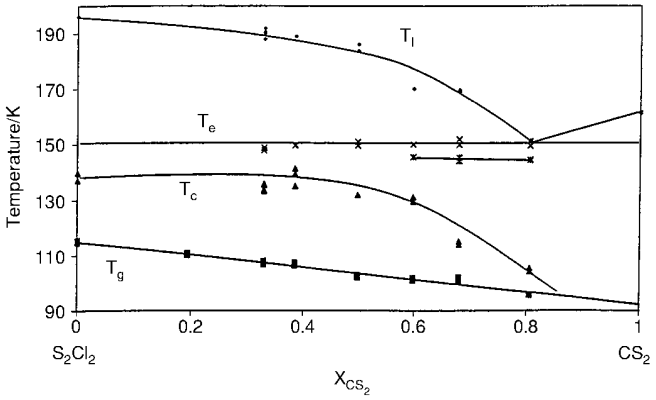

Fig. 2 Glass-forming composition region and glass transition temperatures for the molecularly simple system sulfur monochloride +carbon disulfide (S_2Cl_2+CS_2). Stability against crystallization maximizes near 50 mol% CS_2. The system appears to be a simple eutectic, but the endothermic effects below the eutectic temperature are unexplained

The cited measurements [15, 16] were made using differential scanning calorimetry studies and the full glass transition width. Because of S_2Cl_2 corrosivity problems, the present measurements were made in glass tubes using differential thermal analysis, and the transition widths are differently defined, as in Fig. 3. To deal with this difference we use the well studied liquid toluene [14, 17] which has a similar glass transition temperature, (117.5 K) to S_2Cl_2 (117 K) as a fragility calibration standard. An alternative method of obtaining fragilities for molecular liquids by DTA, will be described in a following section.

The reduced transition widths for the binary S_2Cl_2+CS_2 system are shown in Fig. 3. They are seen to be the same for the two end members, each of which have

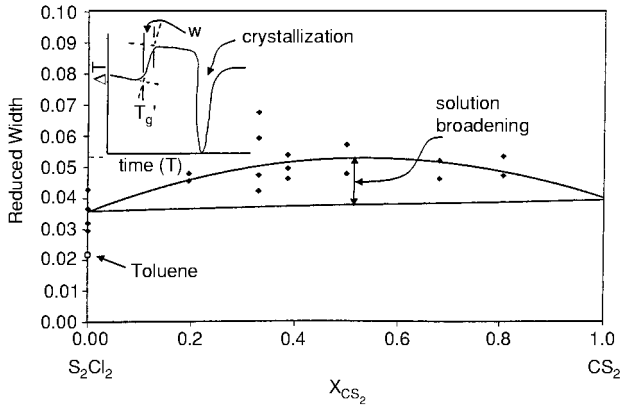

Fig. 3 The reduced widths of the glass transitions in relation to solution composition in the system S_2Cl_2+CS_2. The typical DTA scan through the glass transition up to crystallization, and the defintion of the transition width, is shown in the insert. For fragility calibration, the width, measured with the present setup for for the well characterized liquid toluene, is shown on the left hand axis

widths almost twice that of toluene. Note the presence of a symmetrical broadening of the transitions with solution composition which reaches a maximum at 50 mol%. We assign this to the effect of a distribution of environments, natural to any solution, with different values of T_g, rather than to any increase of fragility with mixing, and will discuss it in a later paper [10].

The end member widths may be scaled to the new $F_{1/2}$ fragility scale (see section 2.1.1) using the value for toluene $F_{1/2}$=0.73 (or 73% fragile). In this way we obtain the value of $F_{1/2}$ (CS_2 and S_2Cl_2)=0.59 or 59% fragile. This value is comparable to that of bromobutane, 0.59 (59% fragile) [18, 19] and is considerably below the values for common fragile glassformers such as propylene carbonate 0.74, oTP 0.71 and CKN 0.75.

To the extent that the molecules CS_2 and S_2Cl_2 approach LJ in simplicity, it would then seem that LJ and mixed LJ systems should behave as moderately fragile liquids only. That it is reasonable to compare the two can be supported by the measured change in heat capacity of S_2Cl_2 at T_g with that of mixed LJ on a per-heavy-atom basis. For S_2Cl_2 the number is 18 J K^{-1} mol^{-1} of atoms [20], while for LJ argon and mixed LJ, measured at a temperature higher than the 'normal' T_g, the ΔC_p value is 16.5 J K^{-1} mol^{-1} of atoms. In each case the heat capacity of the glass is classical (3 R g^{-1}-atom) at T_g.

Elsewhere [8] this heat capacity has been used together with the assumption that there are $e^{\alpha N}$, (α~1), states per mole of heavy particles [21], to argue that the landscape entropy is fully excited by a temperature of 1.56 T_K, or somewhat above the mode-coupling T_c for fragile liquids. (T_c is also the dynamic crossover temperature identified by scaling procedures of Rössler and coworkers [22], and the Stickel temperature identified by derivative data analysis by Stickel *et al*. [23] and the α-β bifurcation temperature.) Since for a bromobutane-like molecule, 1.56 T_K would be close to the T_c value, it would seem from Fig. 1 that this estimate cannot be correct. The total entropy needs to be higher. The temperature characteristic of the top of the landscape $T_{ToL}=E_{ToL}/k_B$ is a strong function of the landscape entropy, so the number of states need only exceed $e^{\alpha N}$ by a small amount e.g. α ~1.5, which is within the estimates. Furthermore, the use of the full ΔC_p at T_g in the integral used to estimate the T_{ToL} is probably incorrect. If part of the observed ΔC_p is assigned to non-configurational sources [24, 25] then, as noted before [8], the T_{ToL} will be shifted to temperatures well above T_c and the latter will be identified more correctly with the peak in the density of states (see section 3).

An important result of this line of thought is that the larger the value of ΔC_p the more rapidly the entropy increases with temperature so the more rapidly the state point will be 'floated' to the top the landscape. Thus the fragile liquids, which are those with higher heat capacities per mole of heavy atoms, have steeper excitation profiles, consistent with the origin of the word 'fragility' as a measure of the rate at which the structure of the liquid evolves (or, rather, 'collapses') with increasing temperature. The corresponding density of states, which is the gradient of the excitation profile, will be narrow in energy. The same result follows from the considerations of section 2.2, in which the steepness of the profile, i.e. the fragility, will be seen to be

determined by a single excitation parameter. Note that the fragility has, until very recently [10, 15], been defined via the behavior of the most obvious liquid property, the viscosity, or some corresponding relaxation time. While we will continue this practice it is important to note here its fundamental thermodynamic origin, which, through the time-dependent fluctuations in equilibrium properties, is then reflected in the relaxation time temperature dependence.

2.1.1. An alternative and unambiguous DTA method for single scan fragility determinations

The conclusion of the previous section is that the liquid fragility is determined by the more fundamental characteristic of the liquid, namely, its density of configuron states. Accordingly, the latter can be determined by appropriate measurements of the former. Therefore it is important to have unambiguous measures of the fragility. We have argued elsewhere [19, 26] that the definitions of fragility currently in use [14, 28–31] are ambiguous, and have proposed a new measure, designated $F_{1/2}$, to minimize the identified problems. Here, in Figs 4 and 5, we will demonstrate a new and direct way to determine $F_{1/2}$ in a single DTA scan.

$F_{1/2}$ is a direct measure of the deviation of the measured system from simple activated Arrhenius behavior with pre-exponent determined by lattice vibrations (implying $\tau_o \sim 10^{-14}$ s). It compares the temperature interval above T_g needed to reach a relaxation time half way (in log units) between low and high temperature extremes, with the corresponding interval in the simple Arrhenius case. Thus it involves no extrapolations, and is determined in a regime where the measurement can be easily made by dielectric, ultrasonic, or light scattering methods and where the deviation from the Arrhenius law is near its maximum for the fragility in question.

Its determination from relaxation time plots in the T_g-scaled Arrhenius representation, has been illustrated in Fig. 1 of [19], and will be seen later in this manuscript in Fig. 6 for the case of viscosity. As seen in those figures the $F_{1/2}$ value is defined by

$$F_{1/2}=2(T_g/T_{1/2}-0.5) \quad (1)$$

(where the quantity inside the brackets is the length l in Fig. 6). Thus it must have values lying between 0 and 1, and can also be cited as % fragile, where 100% fragile would correspond to a first order transition from liquid to glass.

Analysis shows that for a 1% uncertainty in the τ measurement, $F_{1/2}$ would be in error by less than 0.05%, if T_g/T were error-free. However, the T_g measurement is probably the greatest source of uncertainty, in which case $F_{1/2}$ is determined by our method within only 1%.

To determine this fragility number in a single measurement, using only a differential thermal analysis set-up for detection, we make use of the relation between the imaginary part of a frequency-dependent response, and energy dissipation [26]. The energy dissipated from a fluctuating field, in a material which the field is perturbing, is a maximum when the field frequency (in radians/s) is the inverse of the most probable relaxation time of the material. This is the condition $\omega\tau=1$ for an exponentially

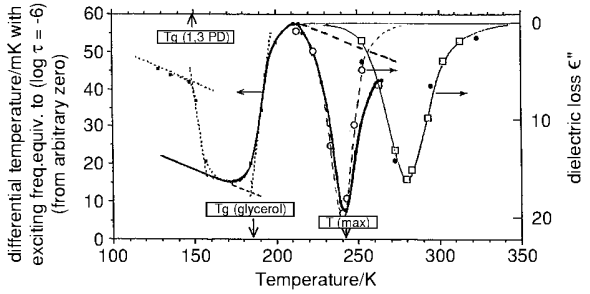

Fig. 4 DTA scans of glycerol with and without irradiation of sample at $10^{5.2}$ Hz showing excitation-induced thermal effect maximizing at temperature where sample has a relaxation time of 10^{-6} s. The thermal effect is almost coincident with the plot of dielectric loss under temperature scanning at a constant frequency of $10^{5.8}$ Hz taken from the work of Morgan. o – [33] –5.8; □ – [33] –8.3; • – [26] –8.3

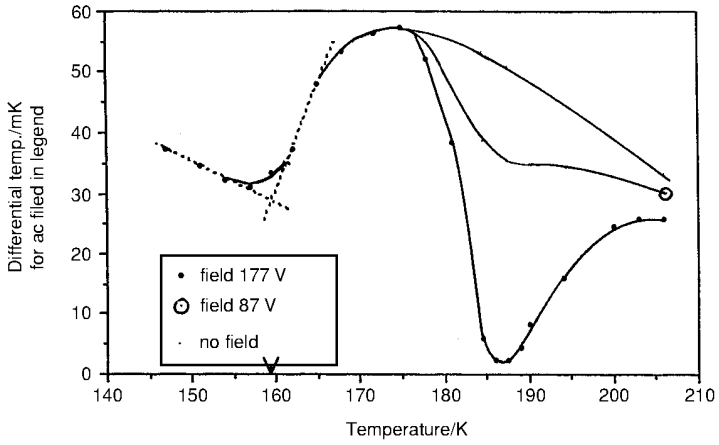

Fig. 5 DTA scans of propylene carbonate under $10^{5.2}$ Hz irradiation at different field strengths, showing growth of excitation induced thermal peak with increasing field

relaxing material, or $\omega\tau^*=1$ for the non-exponentially relaxing case (τ^* being the most probable relaxation time). Therefore, during a temperature scan, the temperature difference ΔT between a sample subject to irradiation at $10^{5.2}$ Hz, and a reference sample of the same substance, will pass through a maximum when the relaxation time of the sample is 10^{-6} s. Thus $T_{1/2}$ of Eq. (3) is obtained as the temperature at the ΔT maximum. The fluctuating field can be of electrical or mechanical origin, though it is simpler to implement in the dielectric case and is also then less likely to promote crystallization of the supercooled liquid.

This method of determining the dielectric relaxation time was demonstrated in 1976 by Matsuo *et al.* [32] but little utilized since. We re-apply it here, and show also, with the help of a commercial ultrasonic agitator operating at 20 kHz, that a similar effect can be obtained by mechanical relaxation. For the dielectric case, the temperature at which the differential temperature is a maximum will be the $T_{1/2}$ of

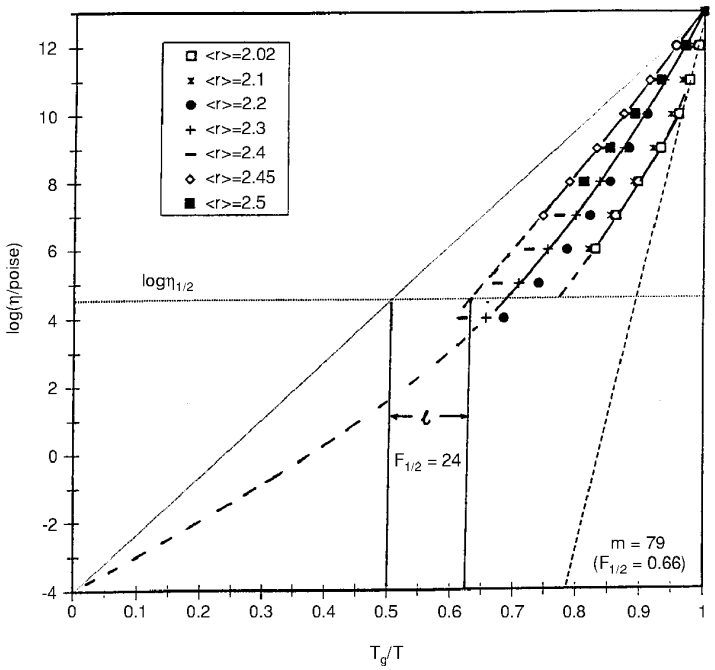

Fig. 6 T_g-scaled Arrhenius plot of viscosity data for Ge+Se melts, showing the wide range of fragilities exhibited as the bond density is changed. Graph shows definition of the 'steepness index' *m* and the preferred fragility metric, $F_{1/2}$ [8, 19, 26], ($F_{1/2}$=21). Pure Se shows *m* and $F_{1/2}$ values which are not consistent, evidently due to special structures near T_g

the $F_{1/2}$ definition, Eq. 1. For the mechanical case using 20 kHz excitation it will be a lower temperature.

If the reference is calorimetrically inert then the glass transition will be recorded in the same scan. If the scan is conducted at 10 K min^{-1}, the value of T_g will correspond to $T_{(\tau=200\ s)}$, and the scan will record both the temperatures needed to define the $F_{1/2}$ fragililty. $T_{1/2}$ will not be affected by the scan rate in principle, since the liquid is in equilibrium at this temperature, though distortion could follow from differences in heat flow. To avoid these we used, as the reference, a liquid with similar heat capacity but lower T_g, (in which case both glass T_gs are recorded during the scan).

The energy dissipation in Joules s^{-1} cc^{-3} from an electric field of RMS voltage E_o acting on a medium of dielectric loss ε'' is given by [32]

$$W(\text{J s}^{-1}\ \text{cm}^3) = E_o^2 \varepsilon'' \omega e_o \qquad (2)$$

(where e_o is the permittivity of free space), and a quick calculation shows that voltages between 20 and 200 V (still well within the linear response regime) are sufficient to generate the heat necessary to detect with a standard DTA set-up.

We used a two pen millivolt recorder and include a low noise operational amplifier (earthed to the recorder) to boost the microvolt DTA differential signal. To produce up to 1200 V(rms) at $10^{5.2}$ Hz we used a FET Hartley oscillator with a one stage buffer followed by several stages of amplification. The field is introduced either externally to the sample via two Al foil electrodes on the outside of the sample tube (as described in [32]), or internally via two metal electrodes attached to the thermocouple sheath.

Results are illustrated for the case of anhydrous glycerol in Fig. 4. The solid line is the DTA scan. To avoid confusion, the reference sample glass transition has been omitted in drawing the solid line (but is shown by the dotted line). Figure 4 shows a glass transition at 185 K and a sharp ΔT maximum at 242 K which is, therefore, $T_{1/2}$ for this substance. Our ac field-induced DTA peak at 242 K is compared with the dielectric loss peak obtained during temperature scan at a constant 100 kHz probe frequency, by Morgan [33]. This frequency will give rise to a maximum loss when $\log\tau$=–5.8, close to our chosen value. The close similarity to our DTA trace is a consequence of Eq. (2) for the energy dissipation. The additional curves in the figure are reliability checks of Morgan's early work discussed in the caption of Fig. 2 of [26].

In the case of a fragile liquid like propylene carbonate, the $T_{1/2}$ energy dissipation peak must occur much closer to T_g and some overlap with the T_g endotherm could become a problem. This can be dealt with by adjusting the exciting field voltage to provide $T_{1/2}$ loss peaks of different magnitudes relative to the pen displacement at T_g. This is illustrated for applied peak-to-peak voltages 0, 87.4 and 176.8 V, in Fig. 5. Equation (2) shows that the heat output should vary as the square of the applied field, though we see less than a factor of 4 difference in ΔT.

The $F_{1/2}$ fragilities of glyercol and propylene carbonate obtained from Figs 4 and 5 are 0.55 and 0.72, respectively. These are to be compared with values of 0.56 and 0.74 obtained from previous dielectric studies in which T_g has been taken as the temperature at which τ=100 s [19]. This may lead to small difference from our values since T_g obtained at scan rates of l0 K m^{-1} in from DTA or DSC tends to occur at 2–500 s [9]. The values which would be predicted from the recorded m values [28] are 0.54 and 0.73, an agreement which is quite pleasing. The combination of this method, with the simpler but less definitive glass transition width measurement discussed in section 2.1, should make the future determination of excitation profiles for supercooled liquids a straightforward matter.

It now remains to examine a second type of simplicity in glassformers – a simplicity which has the advantage that it provides the basis for description of the phenomenology by simple models which in turn permit a straightforward evaluation of the excitation profiles for liquids of different fragility.

2.2. Excitationally simple glassformers

In this section we deal with systems in which it is reasonable to assume that most of the thermodynamics, hence also [1] the main features of the dynamics, are determined by the breaking of well defined bonds. Then it is possible to transpose from the strongly interacting particle lattice to the weakly interacting 'bond lattice' and in

first approximation treat the bonds as independently excitable [34]. In a case like the Se-rich Ge–Se alloys that we consider here, the two relevant bonds are of almost equal energy, simplifying even further the treatment. Experiment will tell us that the excitation parameters descriptive of this simple system depend dramatically on the distribution of bonds between the particles.

2.2.1. Fragility minima in covalent glassformers

We start with an examination of a set of viscosity data for the Ge–Se system by Nemilov [35] because they extend far enough above T_g for the $F_{1/2}$ fragilities to be determined directly. They are shown in Fig. 6 using the T_g-scaled viscosity plot which has become familiar in recent years [1, 14, 36]. It is immediately clear that a wide range of fragilities is manifested in this system as the composition changes.

The $F_{1/2}$ fragility [19] is assessed for the composition of maximum strength $r>=2.45$, using the construction shown, ($F_{1/2}$=2l) and found to be 0.24, comparable with that of sodium disilicate. For higher and lower selenium contents, the fragility decreases. The data for pure Se show an anomaly[1], presumed due to the ring-chain complexity of this substance.

We now confirm the trend of fragility with composition using the measure of the glass transition width, as done earlier for the molecular glasses in Fig. 3. The results are shown in Fig. 7 and confirm the trend seen in Fig. 6. The fragility for Se indicated by the width measurement is consistent with the steepness index measure

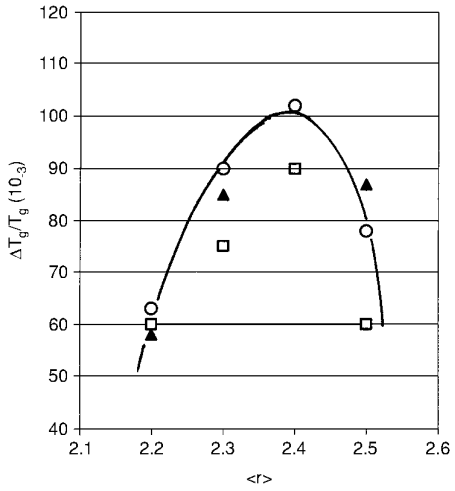

Fig. 7 Reduced width of the glass transition for Ge–Se alloys of different Ge content (i.e. different average bond densities, <*r*> from this work as [60]. Note maximum at expected rigidity percolation threshold, <*r*>=2.4. o – DSC [60]; □ – DSC; ▲ – DTA

1 The $F_{1/2}$ fragility assessed at log (η/p)=3.5, is 0.54, which is much smaller than that obtained from the steepness index m=79 (Fig. 5), via the relation $F_{1/2}=(m-16)/(m+16)=0.68$ (7). This is unusual, and implies a serious breakdown in the VFT equation for this substance.

rather than the direct $F_{1/2}$ measure, for the obvious reason that it is conducted near T_g where the steepness index is determined.

We could, logically, now discuss the origin of the fragility minimum at <*r*>=2.4–2.45, in terms of the 'rigidity percolation threshold' described by Phillips, Thorpe, and coworkers [37–39]. However this has been done adequately elsewhere [10, 40]. Instead we proceed directly to a simple theoretical description of the observations in order to show how the excitation spectrum of Fig. 1 can be reproduced, based on the independent bond approximation.

2.2.2. The bond lattice model and the excitation profile

The number of bonds per mole of atoms depends on the chemical constitution, via the 8-n rule (*n* the periodic table group number) for single covalent bond formation. Since each bond links two atoms, the number of bonds in the bond lattice is one mole per mole of Se, and two moles per mole of Ge, these numbers setting the range for the systems considered here. We assign an enthalpy of bond breaking of ΔH^* and an associated entropy change ΔS^*. We will be specially interested in ΔS^*, because it determines the fragility, as will be seen. Then, treating the Se–Se and Se–Ge bonds as equivalent in energy, the fraction X_B of bonds broken at temperature T is given [34] by the usual two-state thermodynamic expression,

$$X_B = [1 + \exp(\Delta H^* - T\Delta S^*)/RT]^{-1} \tag{3}$$

and the associated heat capacity is

$$C_p = (\partial H/\partial T)_p = R(\Delta H^*/RT)^2 X_B(1 - X_B) \tag{4}$$

In the simple magnetic systems for which this type of behavior was first described, ΔS^* is zero because the flipping of a spin causes no entropy change other than that associated with the distribution of different spins among the N atoms in the structure. Then Eqs (3) and (4) give rise to smeared out heat capacity bumps with a maximum value of ~1 cal mol^{-1} K^{-1}, known as Schottky anomalies. Almost the same situation appears to hold in an optimally constrained bond lattice, as will be seen. However, in under-constrained (and also, it seems, in over-constrained systems) the breaking of a single bond can give rise to more entropy than is indicated by the standard distribution across the bond lattice. This extra entropy is recorded as the ΔS^* of excitation in Eq. (3). ΔS^* may be due to a local structure degeneracy, y, introduced on bond breaking, $\Delta S^* = R\ln y$, or may be vibrational in character, arising because the excitation is accompanied by a decrease in average vibration frequency for the quasi-lattice region containing the 'defect' ($\Delta S_{vib} = R\ln(\nu_2/\nu_1)$). The elucidation of this physics is shown, by the present analysis, to be a crucial component of the 'glassy state problem'.

In view of the importance of this issue, we note that in a somewhat analogous case, the excitation of interstitial defects in crystal lattices, the generation of low frequency vibrational modes accompanies defect formation, and provides a strong en-

tropic drive to increase the defect population [40]. We suspect that a similar phenomenon may be the source of the well-known but poorly understood quasi-elastic neutron scattering intensity build-up in glassformers above T_g. It is, in this case, no surprise that this intensity build-up is most striking in the case of fragile liquids, since this must imply a larger ΔS^* for such cases.

When ΔS^* is non-zero, the heat capacity bump is sharpened in proportion to ΔS^*, as shown in Fig. 8(a). For the case of Ge–As–Se at the bond density 2.4, the maximum heat capacity rise is only about 1 cal $mol^{-1}K^{-1}$ (Fig. 8(b)) which is the Schottky anomaly value, corresponding to $\Delta S^*=0$. In this limit the glass transition reduces to a problem of minor interest, a kinetically arrested Schottky anomaly. From the above

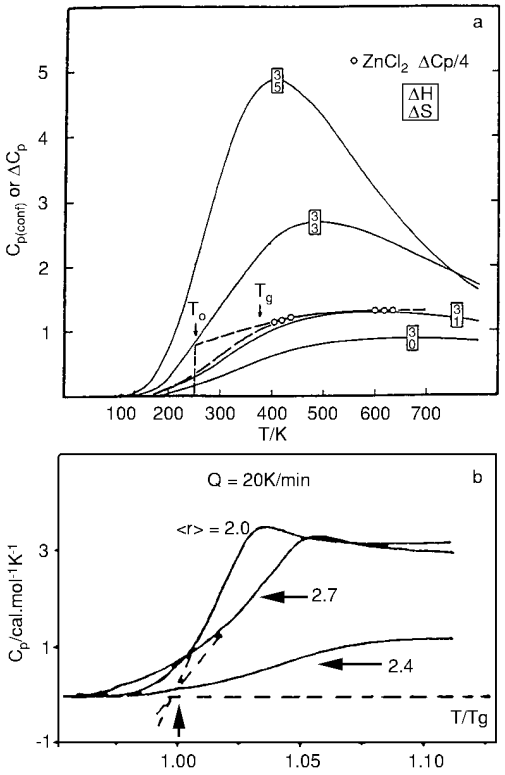

Fig. 8 a – Variation of the heat capacity with temperature according to Eq. (11) for the parameter sets indicated alongside the curves. Comparison is made with the case of $ZnCl_2$ for data obtained near the glass transition temperature and above the melting point, and the deviation of the theoretical curve from that assumed in calculating the Kauzmann temperature for this substance [48], is noted. The assessment assumes four breakable bonds per mole of $ZnCl_2$ [25].
b – Excess heat capacities (over the glass values) of Ge–As–Se alloys of different average bond densities, as function of reduced temperature (scaled by the respective glass transition temperatures). Note that the excess for the bond density 2.4, when reduced to the value per mole of bonds (factor of 1.2^{-1}) is the Schottky anomaly value at the maximum of the heat capacity (see part (a))

discussion, we would predict very little quasi-elastic scattering build-up above T_g in this case. Conversely, high heat capacity jumps at T_g for Se and also for compositions with $<r>>2.4$ (Fig. 8(b)) must be a direct consequence of a large constraint-breaking entropy increment, ΔS^* of Eq. (3). ΔS^*, in other words, determines the excitation profile, hence the temperature range over which the configuron states are excited. In this case it is important to make comparisons with the excitation profile for molecularly simple systems.

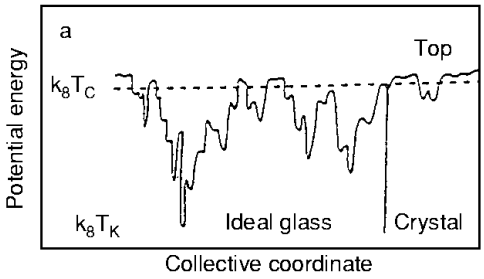

Fig. 9 a – The 2D representation of the energy 'landscape' for a system of interacting particles, indicating the relation between crystal, liquid and 'ideal glass' states. The figure suggests that the 'top of the landscape' falls near the mode-coupling critical temperature which is only the case for well of depth $<kT$

The excitation profile obtained for the mixed LJ system and shown in Fig. l was obtained from simulations conducted at constant volume [2]. For comparisons with such a case we would use Eq. (3), with ΔE^* in place of ΔH^*. The energy excitation profile is then obtained as the product of ΔE^* and the fractional excitation X_B of Eq. (3). Its form is shown by the plot of X_B *vs.* T which, in Fig. 9, is compared with the profile obtained from the computer quench studies of Fig. 1. Considerable similarity is evident, which we discuss after brief comments on how the bond lattice model relates to liquid relaxation processes.

2.2.3 Relaxation in the liquid state

In [34] it was argued that the probability of a rearrangement of atoms, such as is needed for a fundamental diffusive event or flow event to occur, must depend on the presence of a critical fluctuation in the local concentration of broken constraints. Invoking the Lagrangian undetermined multipliers treatment of constrained maxima [42], this probability is found to be an exponential function of the fraction of broken constraints at each temperature. This gives rise to a three-parameter expression for the temperature dependence of the relaxation probability $W(T)$

$$W(T) \sim \exp(f^*/X_B(T)) \tag{5}$$

where f^* is a critical local broken constraint fraction and X_B is the overall broken constraint fraction, determined by the two parameters ΔH^* and ΔS^* of Eq. (3). Because X_B is linear in temperature over much of the range, Eq. (5) yields the Vogel-

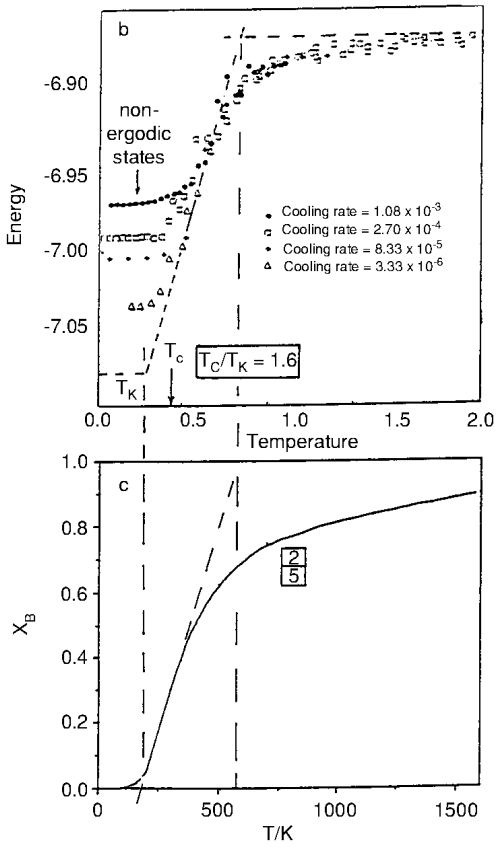

Fig. 9 b – The relation between the portion of the energy landscape visited by the system most frequently, and the temperature of the system, according to recent MD computer simulation inherent structures studies [2]. To obtain the ergodic behavior at lower temperatures, the profile has been extrapolated linearly to the temperature T_K according to the relation T_c/T_K=1.6 observed for a variety of fragile liquids in laboratory studies T_c, according to the MD studies of Ref. [39], is 0.435 in Fig. 8(b) units. The 'width' of the profile defined by the linear extrapolation of the steep part of the profile to the ground state and to the 'top' respectively, is indicated by vertical dashed lines
c – The Eq. (3) excitation profile for parameters (in box) and T units which approximately match the width of the mixed LJ system profile of Fig. 8(b). For Eq. (3), the 'top' of the excitation profile is only reached at T=∞. The general similarity of the Fig. 8(b) and Fig. 8(c) excitation profiles can be taken to advantage to simplify the description of liquid properties which are necessarily complex in multidimensional energy landscape terminology. Note the ergodic behavior near T_K. The gradient of the excitation profile gives a measure of the density of configurational states for the liquid

Fulcher equation. It turns out that the slope B is proportional to the (extrapolated) temperature of vanishing excitation, T_o, yielding

$$\tau = \tau_o \exp(DT_o/(T - T_o) \quad (6)$$

where the strength parameter D is determined by the parameters ΔS^* and f^*, and T_o is determined solely by the parameter ΔH^*. Thus there are simple connections between the excitation profile and the relaxation time temperature dependence, i.e., the kinetic fragility. f^* requires a value of about 0.2 to give a relation between thermodynamics and relaxation time which is consistent with experiment. For example, the maximum D value will be found for the case in which ΔS^* is zero, and the slope dX_B/dT is a minimum. From [43], this is found to be 83, which requires $f^*=0.13$.

3. Comparison of excitation profile for simple mixed LJ system (Fig. 1), with profiles from the bond model

In section l, Fig. 1, the excitation profile was depicted as a plot of the energy of the (mixed LJ) system, equilibrated at temperature T, that is retained when the non-configurational energy is suddenly removed by a procedure which assured that the system was trapped directly in the 'landscape' minimum above which it was located at the moment of quench. Repeat runs assure that, even for the small system under study, the energy of this minimum is confined to a small band for each temperature below the value ~1.0 in system units. The understanding is that this is the value of energy E to which the system is driven by the TS product in the Helmholz free energy $A=E-TS$, where S is given by the sum of $k_B \ln W$ (W being the number of minima to which the system has access) plus any additional vibrational entropy $\Delta S=R\ln(\nu_2/\nu_1)$ that might accompany configurational excitation.

In terms of the bond model the system is driven to a given state of configurational excitation (X_B) by exactly the same factors, and so the excitation profile should be given directly by the equation for X_B. The configurational energy for an isochoric system would be simply the $X_B\Delta E^*$ product. We can therefore make a direct comparison of the profile obtained by configuration space considerations on the one hand, and by simple elementary excitations arguments on the other.

3.1. Excitation profiles and densities of configuron states

The relation between the excitation profile from simulations on mixed LJ (Fig. 1) and that calculated using Eq. (3), with parameters chosen to give the same 'reduced width' as for LJ, is shown in Fig. 9. The reduced width is the ratio of temperatures obtained by extension of the steep linear part of the excitation profile to the 'top of the landscape' of panel 2 on the one hand and to the ground state level[1] on the other

1 We note again [34] how the bond lattice treatment in the 'independent bond' approximation, denies the existence of a finite Kauzmann temperature, though shows how an operationally defined ground state temperature (which would be the T_o of Eq. (6)) is obtained by short extrapolation of the excitation profile. The double exponential equation, Eq. (5), fits transport and relaxation time data as well as does Eq. (6) [44] without requiring a finite ground state temperature. However, it was shown in [34] that the glass transition phenomenon in fragile liquids is significantly sharper than can be accounted for by Eq. (10) and it is possible that cooperative effects, neglected in the zeroth order model, may produce a genuine singularity in principle though there is yet no evidence for it. The possibilities are illustrated in [45].

(see the vertical dashed lines in panels (b) and (c) which delineate the 'widths'). The top of the landscape in panel (c) is the high temperature limit of X_B and corresponds to the excitation of the full landscape entropy of approximately R entropy units per mole of particles [46].

The resemblance of the excitation profiles for the mixed LJ system, (panel (b)) and the simple two state model (panel (c)) is quite impressive and, we think, instructive considering their very different derivations. The implication is that any instantaneous collection of bond lattice excitations represents a configuration space minimum, and can be 'frozen in' for evaluation by conjugate gradient quenching. This is of course the starting premise in any two-state treatment viz. that the vibrational excitations of the particle lattice are separable from the configurational excitations of the bond lattice. The separability depends on the same difference in relaxation times which makes the quenching-in of a particular configuration possible.

The Eq. (3) profile approaches the fully excited limit more gradually than does the LJ system. There is more of a 'shelf' before the plunge to the configurational ground state. This difference may be associated with the constant value assumed for ΔS^*. If an important part of ΔS^* comes from the generation of low frequency modes in the vibrational density of states (being revealed as the quasielastic scattering intensity build-up in neutron scattering studies) then it is not unreasonable to suppose that the new vibrational modes excited should become lower in frequency as the structure becomes looser, thus accelerating the drive to full excitation as seen in Fig. 9(b).

Note that we have had to invoke a rather large excitation entropy in order to match the width of the mixed LJ profile defined as in Fig. 8 panel (b). The $\Delta C_{p,max}$ value corresponding to this ΔS^* value is (Fig. 7) 4.8 cal mol^{-1} K^{-1} which corresponds closely with the mixed LJ value for ΔC_p at the *MD* glass transition, namely 4.3 cal mol^{-1} K^{-1} [47] if there is only one constraint per particle. The corresponding D value, ($D=B/T_o$) according to Fig. 6(b) of [34], should be approximately 3 for $f^*=1.0$, *c.f.* $D=8$ near T_g for Se, the most fragile liquid in Ge–As–Se system. The value 3 is characteristic of a very fragile liquid [1] as would be expected at first thought for mixed LJ. However we have seen in section 2.1 from data on molecularly simple systems, that mixed LJ is probably only a moderately fragile liquid and therefore a value of D more like 10 would be expected. Thus again a value of f^* (Eq. (5)) well below 0.5 is indicated. If the profile of Fig. 1 (and Fig. 9(b)) is that of a moderately fragile liquid, then we must ask what is to be expected for the profiles of very fragile liquids on the one hand, and very strong liquids on the other. Here the bond model has simple answers if independent bonds are assumed and interesting answers if non-random bonding is introduced. The latter case is considered in a final section.

In more fragile systems the liquid is driven to full excitation more quickly by the presence of larger excitation entropy ΔS^* values. Also the inflection point in the profile will occur at higher excitation fractions, (particularly if ΔS^* is allowed to be dependent on the state of excitation, as discussed above). Irrespective of the source of the excitation entropy the excitation profile tells us the temperature range over which the landscape microstates become populated hence indicates the density of configu-

rational states. Quantitatively this *DoS* should be obtained from the gradient of the profile.

Stronger liquids will be those whose excitation profiles are widely spread in temperature and such liquids may pass the melting points, and even the boiling points, of the liquids before they reach the 'tops of their landscapes'. Thus the intermediate liquid $ZnCl_2$, which in fact shows the presence of the C_p maximum predicted by Eq. (4) [34], will melt while the landscape is only partly excited. Indeed, the entropy of fusion is less than R entropy units per mole of heavy atoms (measured value is 0.66 $R\ g^{-1}\ atom^{-1}$ [48]). Likewise SiO_2,which melts to give the strongest liquid known (except for glassy water), melts with much less than R entropy units per mole of heavy atoms (measured value is 0.37 $R\ g^{-1}\ atom^{-1}$).

In the fully covalent systems, this broadest density of states is realized for compositions with optimized bond densities, $<r>=2.4$, since it is at this composition that the excitation entropy approaches zero, as we have seen earlier.

3.2. Excitation profiles and 'crossover' phenomena

Many workers have drawn attention to the existence of some sort of change of mechanism in transport for fragile liquids at a temperature of about l.2 T_g. The most direct indication of this is the familiar bifurcation of the relaxation process into α- and β-processes which is observed at a relaxation time in the vicinity of 10^{-5}–10^{-7} s. This occurs at the same temperature as the relaxation time divergence of Mode Couping theory [50]. Other indicators are the break in the Stickel plot for relaxation time temperature dependence between two apparently separate VFT domains [22, 51], the temperature of breakdown of the Stokes-Einstein equation [50] the crossover temperature of the Rossler-Sokolov viscosity scaling [23], and most recently, the temperature of breakdown of the Adam-Gibbs equation [19]. For a given liquid, all these temperatures have the same value: it falls at a value of T_g that depends on the fragility.

The position of the mode coupling theory T_c [2, 6] on the profile of the mixed LJ system, Fig. 9(b) is therefore of interest. It is more than half way down to the ground state energy, and close to the inflection point of Eq. (3) seen in Fig. 9(c). This is consistent with the observations of Fischer [49] who fitted equations based on a two-state model to the experimental data for several molecular liquids for which T_c had been determined by other workers. (It is below this energy that most of the many orders of magnitude change of relaxation time occur en route to the glass transition.) Thus an interpretation of the 'crossover' phenomena could be given in terms of passing through the maximum in the density of states. The departure from near-linearity in temperature of the function X_B which is the denominator of the relaxation probability expression, provides (via Eq. (5)) a rather direct explanation for the failure of the Vogel Fulcher equation near T_c. This is very different from the suggestion of one of us [46] and of Sokolov [52] that the crossover is due to arrival at the 'top' of the landscape. Rather it corresponds to arrival at the upper regions of the landscape where wells have depths less than kT [53], and escape is therefore always possible without activation.

From the Fig. 9 comparison, we can then go on to describe at least qualitatively, the energy landscape excitation profiles for chalcogenide liquids of different <*r*> values using the fragilities measured in [43] and the Eq. (3) 'excitation profiles' for the associated bond-breaking parameters ΔH^* and ΔS^*. This analysis will be presented in more detail when a study of the simple two-component system Ge–Se, currently in progress, has been completed.

3.3. Non-random bonding and liquid-liquid phase transitions

Of additional interest in the chalcogenide systems is the existence of a maximum T_g value as Ge content increases and the system becomes severely overconstrained. The existence of a general maximum can be deduced from the knowledge that the diffusivity of crystalline Ge exceeds that characteristic of a substance at its glass transition (10^{-22} m^2 s^{-1}) at 550 K [54] so that amorphous Ge must presumably have a T_g value no higher than 550 K. (This is close to its observed recrystallization temperature). The maximum has been directly observed in the case of the Ge–Se system [55, 56] and can be associated with an effective reduction of the Ge oxidation state towards +2 (GeSe). A T_g of 550 K is reached at 35% Ge in the binary system $GeSe_2$ [56] and should be realized in any cut through the ternary system at comparable Ge fractions. Although it has not been reported to date, this would probably be followed by the splitting out of a pure Ge phase with about the same T_g value. In this domain the independent constraint-breaking assumption made in the two-state treatment we have given must break down, and interesting analogies with the landscape interpretations of polyamorphism [45] will present themselves.

In the maximally over-constrained cases, Ge and Si, first order liquid-liquid phase transitions are believed to occur [57]. They have been observed in detail in computer simulation studies of Si [58]. These can be explained if the bond-breaking is taken to be cooperative in the sense of A+B regular solutions. Then a composition with a critical point will exist, and beyond that composition the sigmoid excitation profile of Fig. 9(c) will become an 'S' – shaped curve – meaning that two states of excitation can co-exist at the same temperature. These will be the high and low density phases of liquid Si (and Ge) identified by laser fusion [57] and computer simulation [58] studies, and discussed in relation to protein folding in [59].

* * *

This work has been carried out under the auspices of the NSF under Solid State Chemistry grant no. DMR 9614531. The authors have benefited from helpful discussions with Burkhardt Geil and Robin Speedy, and particularly Paul Madden who drew our attention to [41].

References

1 C. A. Angell, J. Non-Cryst. Sol., 13 (1991) 11.
2 S. Sastry, P. G. Debenedetti and F. H. Stillinger, Nature, 393 (1998) 554.
3 F. H. Stillinger and T. A. Weber, Science, 225 (1984) 983.
4 C. A. Angell, J. H. R. Clarke and L. V. Woodcock, Adv. Chem. Phys., 48 (1981) 397.
5 H. Jonnson and H. C. Andersen, Phys. Rev. Lett., 60 (1988) 2295.

6 W. Kob and H. C. Andersen, Phys. Rev. E., 51 (1995) 4626.
7 W. Kauzmann, Chem. Rev., 43 (1948) 219.
8 C. A. Angell, in 'Complex Behavior of Glassy Systems' (Proc. l4th Citges Conference on Theoretical Physics, 1966) Ed. M. Rubi, Springer, 1967, p. 1.
9 C. A. Angell, Proc. Int. School of Physics, 'Enrico Fermi' Course CXXXIV edited by F. Mallamace and H. E. Stanley, IOS Press, Amsterdam 1997, p. 571.
10 C. A. Angell, B. E. Richards and V. Velikov, J. Phys. Condensed Matter, 11 (1999) A75.
11 Y. Choi, M. Sc. Thesis, Purdue University, 1984.
12 Handbook of Chemistry and Physics, 76th Ed. CRC Press, 6-245, 1995.
13 W. T. Laughlin and D. R. Uhlmann, J. Phys. Chem., 76 (1972) 2317.
14 C. A. Angell and W. Sichina, Ann. N.Y. Acad. Sci., Vol. 279, (Proc. Workshop on the Glass Transition and the Nature of the Glassy State) (1976), p. 53; C. A. Angell in Relaxations in Complex Systems, ed. K. Ngai and G. B. Wright, National Technical Information Service, U.S. Department of Commerce, Springfield, VA 22161, 1985, p. 1.
15 K. Ito, C. T. Moynihan and C. A. Angell, Nature, 398 (1999) 492, K. Ito, C. A. Angell and C. T. Moynihan (to be published).
16 C. T. Moynihan, J. Am. Ceram. Soc., 76 (1993) 1081.
17 L. Wu, Chem. Rev. B., 43 (1991) 9906.
18 M. Baranek, M. Breslin and J. G. Berberian, J. Non-Cryst. Sol., 172-174 (1994) 223.
19 R. Richert and C. A. Angell, J. Chem. Phys., 108 (1998) 9016.
20 C. A. Angell and J. C. Tucker, (to be published).
21 R. J. Speedy and P. G. Debenedetti, Mol. Phys., 86 (1995) 1375.
22 E. Rossler and A. P. Sokolov, Chem. Geol., 128 (1996) 143.
23 F. Stickel, E. Fischer and R. Richert, J. Chem. Phys., 104 (1996) 2043.
24 M. Goldstein, J. Chem. Phys., 64 (1976) 4767.
25 C. A. Angell and J. Wong, J. Chem. Phys., 53 (1970) 2053.
26 J. L. Green, K. Ito and C. A. Angell, J. Phys. Chem., 103 (1999) 399.
27 R. Böhmer and C. A. Angell, Phys. Rev. B., 4 (1992) 10091.
28 R. Böhmer, K. L. Ngai, C. A. Angell and D. J. Plazek, J. Chem. Phys., 99 (1993) 4201.
29 A. P. Sokolov, E. Rossler, A. Kisliuk and D. Quittman, Phys. Rev. Lett, 71 (1993) 2062.
30 E. Donth, J. Non-Cryst. Sol., 53 (1982) 325.
31 I. M. Hodge, J. Non-Cryst. Sol., 212 (1997) 74.
32 T. Matsuo, H. Suga and S. Seki, Bull. Chem. Sol. Japan, 39 (1966) 1827.
33 S. O. Morgan, Trans. Electrochem. Soc., 65 (1934) 109.
34 C. A. Angell and K. J. Rao, J. Chem. Phys., 57 (1972) 470.
35 S. V. Nemilov, Zhur. Prikl. Khim., 37 (1964) 1020.
36 C. Alba, J. Fan and C. A. Angell, J. Chem. Phys. 110 (1999) 5262.
37 M. F. Thorpe, J. Non-Cryst. Sol., 57 (1983) 355; M. F. Thorpe in Amorphous Insulators and Semiconductors, eds. M. F. Thorpe and M. I. Mitkova, NATO-ASI Series, Plenum Press, 1997, p. 289-328.
38 J. C. Philipps, J. Non-Cryst. Sol., 34 (1979) 153; J. C. Philipps and M. F. Thorpe, Sol. State Commun., 53 (1985) 699.
39 H. He and M. F. Thorpe, Phys. Rev. Lett., 54 (1985) 2107.
40 C. A. Angell, in 'Rigidity: Theory and Applications' eds. M. F. Thorpe and P. M. Duxbury, Plenum, (in press).
41 A. V. Granato, Phys. Rev. Lett., 68 (1992) 974; J. Phys. Chem. Sol., 55 (1994) 931.
42 (a) M. H. Cohen and D. Turnbull, J. Chem. Phys., 31 (1959) 1164; (b) H. Van Damme and J. J. Fripiat, J. Chem. Phys., 62 (1978) 3365.
43 M. Tatsumisago, B. L. Halfpap, J. L. Green, S. M. Lindsay and C. A. Angell, Phys. Rev. Lett., 64 (1990) 1549.
44 C. A. Angell and R. D. Bressel, J. Phys. Chem., 76 (1999) 3244.
45 C. A. Angell, Proc. National Academy of Sciences, 92 (1995) 6675: C. A. Angell, P. H. Poole and J. Shao, Nuovo Cimento, 16D (1994) 993.

46 C. A. Angell, APS Symposium Proceedings, J. Res. NIST, 102 (1997) 171.
47 K. Vollmayr, W. Kob and K. Binder, Phys. Rev. B, 54 (1996) 15808.
48 C. A. Angell, E. Williams, K. J. Rao and J. C. Tucker, J. Phys. Chem., 81 (1977) 238.
49 C. H. Wang and E. W. Fischer, J. Chem. Phys., 105 (1996) 7316: E. W. Fischer (preprint).
50 E. Rössler, Phys. Rev. Lett., 65 (1990) 1595.
51 C. Hansen, F. Stickel, T. Berger, R. Richert and E. W. Fischer, J. Chem. Phys., 107 (1997) 22.
52 A. Sokolov, Endeavor, 21 (1997) 109.
53 W. Kob and F. Sciortino (preprint).
54 S. Coffa, J. M. Poate and D. C. Jacobson, Phys. Rev. B., 45 (1992) 8355.
55 See Chapter 3 of A. Feltz, 'Amorphous Inorganic Materials and Glasses', VCH Verlag., Weinheim, N.Y. 1993.
56 A. Feltz and F. J. Lippmann, Z. Anorg. Allgem. Chem., 398 (1973) 157.
57 M. O. Thompson, G. J. Galvin, J. W. Mayer, P. S. Peercy, J. M. Poate, D. C. Jacobson, A. G. Cullis and N. G. Chew, Phys. Rev. Lett., 52 (1984) 2360.
58 C. A. Angell, S. Borick and M. Grabow, J. Non-Cryst. Solids, 205–207 (1996) 463.
59 C. A. Angell, Science, 267 (1995) 1924.
60 L. Leneindre, Thèse, Rennes, 1994.